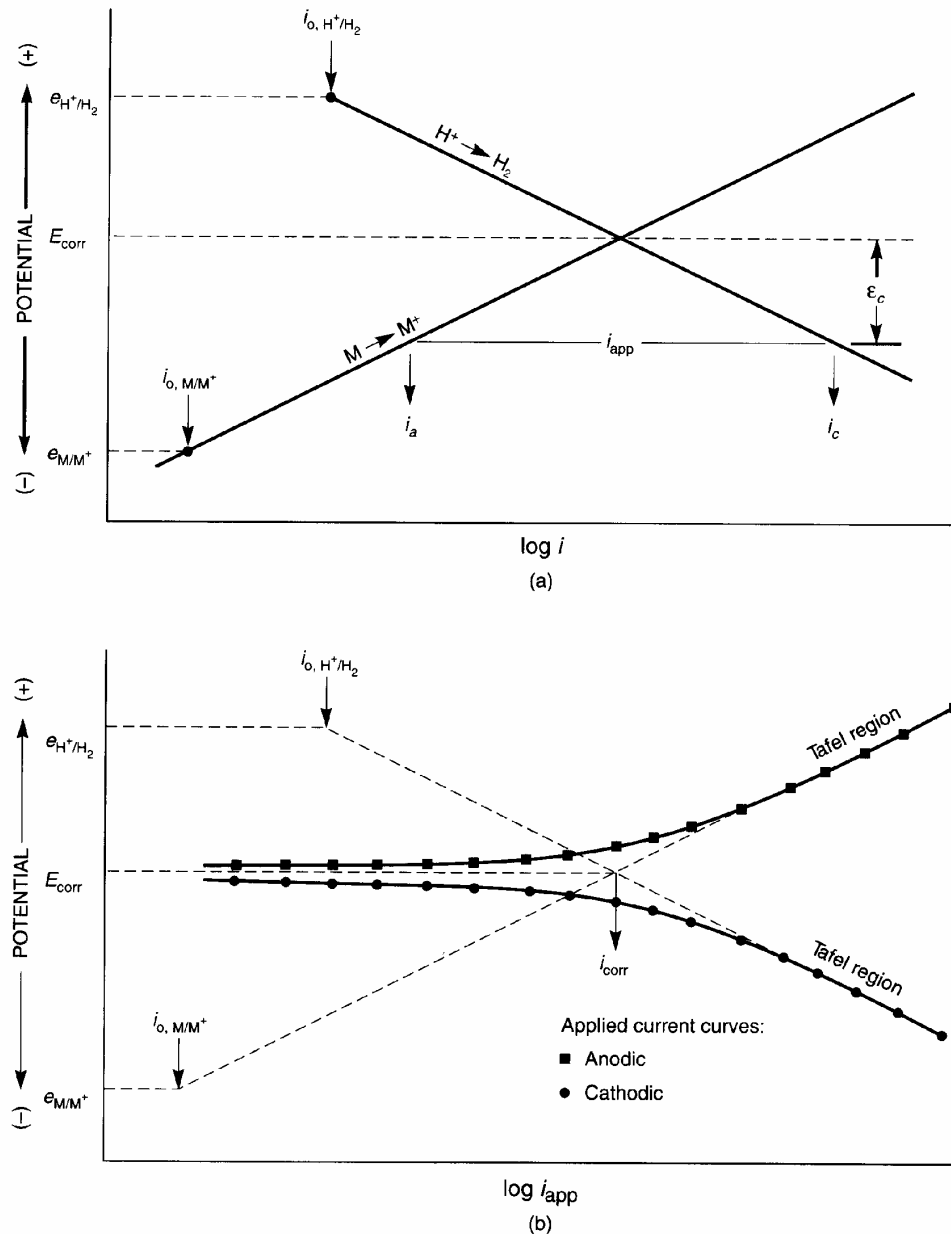


## Cathodic and Anodic Polarization:

When an excess of electron flow is applied to a system with a current density of  $i_{\text{appl, c}}$ , the electrode potential shifts negatively from  $E_{\text{corr}}$  to  $E$ , which can be written as  $\varepsilon_c = E - E_{\text{corr}}$ . This leads to a decrease in  $i_a$  and an increase in  $i_c$ . As we still need an equal charge flow we can calculate  $i_{\text{appl, c}} = i_c - i_a$ . This is shown in figure 3.14a. A similar approach is valid for anodic polarization.



**FIGURE 3.14** (a) Current density,  $i_{\text{appl}}$ , applied to corroding electrode of  $E_{\text{corr}}$  and  $i_{\text{corr}}$ , causing cathodic overvoltage of  $\varepsilon_c$ ; (b) simulated experimental polarization curves derived from (a).

In figure 3.14 b the data points represent  $i_{\text{appl, c}}$  and  $i_{\text{appl, a}}$ , for cathodic and anodic polarization, respectively. With high  $\varepsilon_c$  and  $\varepsilon_a$   $i_{\text{appl, c}}$  and  $i_{\text{appl, a}}$  are large and the points coincide with the Tafel plots, whereas with lower  $\varepsilon_c$  and  $\varepsilon_a$  the measured points start to deviate from the

theoretical behaviour. As can be seen in figure 3.14b one can get  $i_{\text{corr}}$  and  $i_0$  for the two half cell reactions by extrapolation of the linear part, where Tafel behaviour is observed. While this usually works good for the cathodic part, one usually does not get Tafel behaviour from measurements of the anodic part, as shown in figure 3.15. But one can calculate the anodic part from the cathodic measurements.

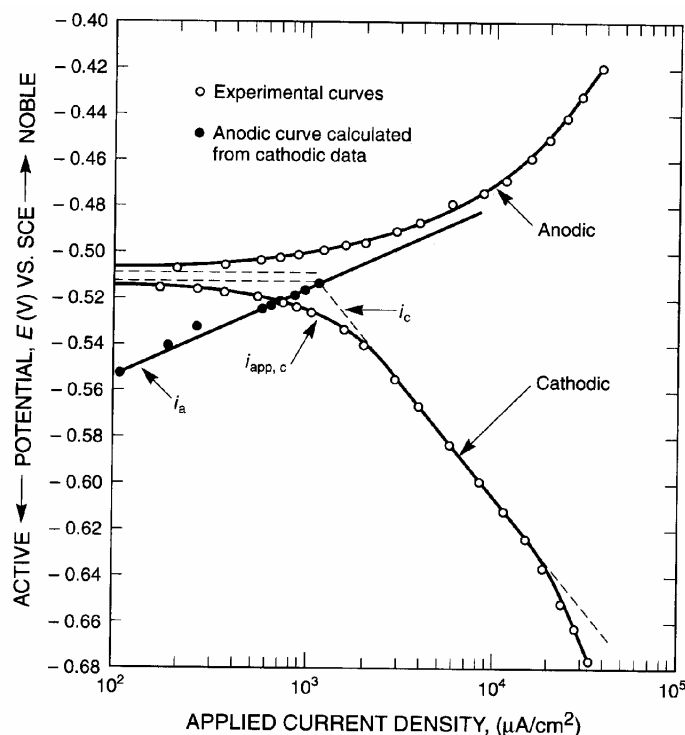


**FIGURE 3.15** Experimental polarization curves for 1080 steel in deaerated 1  $N$   $H_2SO_4$ ,  $\beta_c = -98$  mV,  $\beta_a = 38$  mV (derived from cathodic data),  $i_{\text{corr}} = 1180 \mu A/cm^2$ . (From R. Bandy and D. A. Jones, Corrosion, Vol. 32, p. 126, 1976. Reprinted by permission National Association of Corrosion Engineers.)

An additional problem in interpreting measured data is the effect of concentration polarization. This brings significant additional deviation from Tafel behaviour as shown in figure 3.16.

Only at the lowest pH, which corresponds to the highest  $H^+$  concentration, a nice linear part is observed in figure 3.16. With increasing pH (decreasing  $H^+$  concentration) the experiment is mainly determined by the concentration polarization. At higher pH hydrogen evolution by direct reduction of water occurs  $2H_2O + 2e^- \rightarrow H_2 + 2OH^-$ , which again is linear following Tafel behaviour, as there is of course a very high concentration of water present.

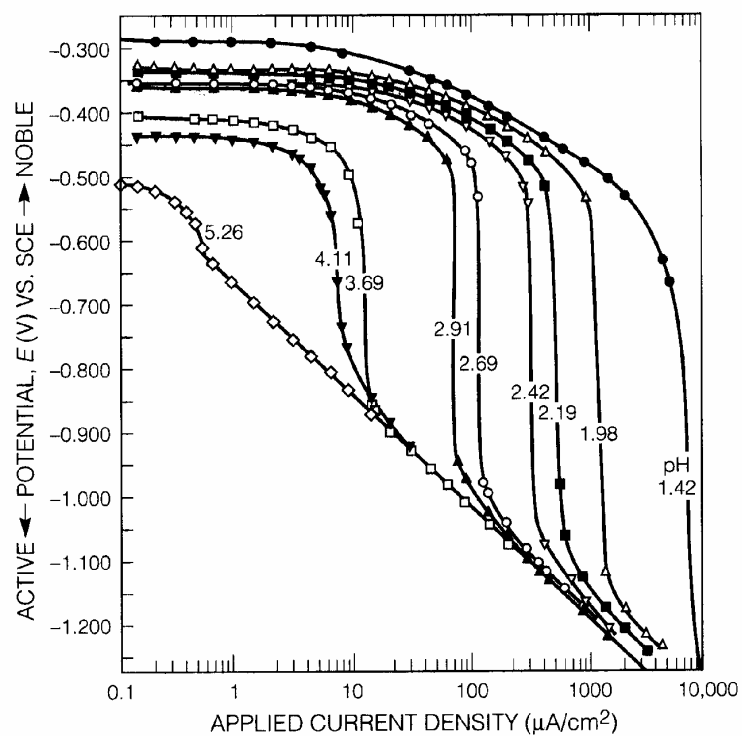
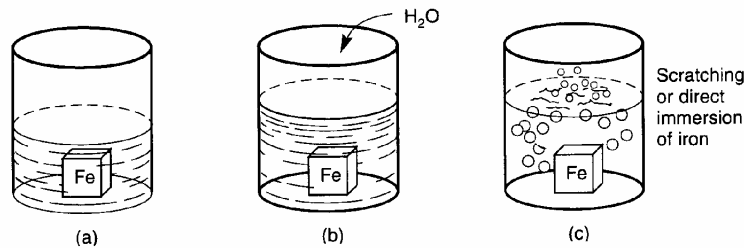


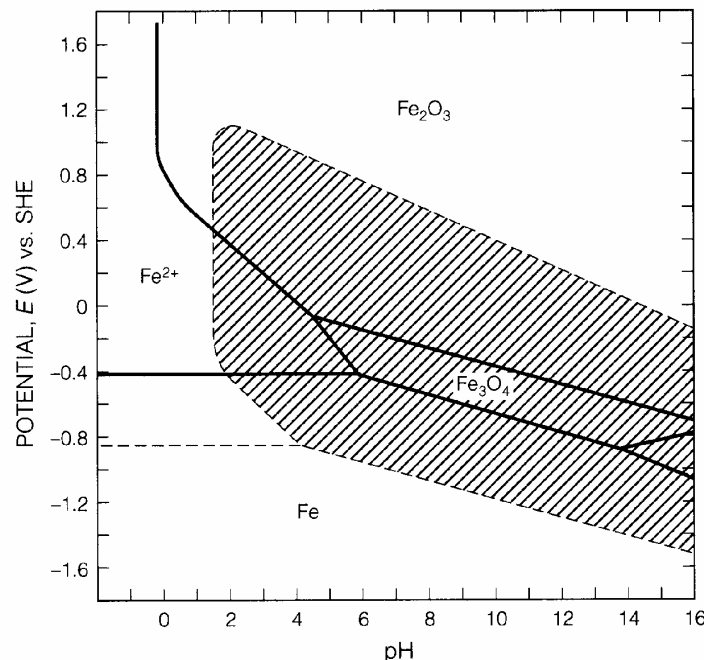
**FIGURE 3.16** Cathodic polarization of pure iron in deaerated 4% NaCl. (From M. Stern, J. Electrochem. Soc., Vol. 102, p. 609, 1955. Reprinted by permission, The Electrochemical Society.)

## Passivity

Passivity is defined as corrosion resistance due to formation of thin surface films under oxidizing conditions with high anodic polarization. For example Fe is passivated in concentrated nitric acid. But in diluted nitric acid Fe is dissolved, or when the passive film is scratched, Fe starts to dissolve, too. This is shown in the following figure.



Fe only passivates in extremely oxidizing environments. The reason is the potential and pH range where iron oxides are thermodynamically stable. This can be seen in the Pourbaix diagram (see figure). Chromium (dashed lines and shaded area) passivates under less oxidizing conditions. But Cr has bad mechanical properties, therefore it is only used as an alloying element in Fe to make stainless steel (min 12% Cr). Ni (> 8%) further enhances corrosion resistance and improves mechanical properties by stabilizing the fcc phase of Fe.



With increasing potential and anodic polarization passive metals show a distinct behaviour. At low potentials corrosion rates measured by anodic current density are high and increase with potential in the active state. Above the primary passive potential  $E_{pp}$  the passive film becomes stable and the corrosion rate decreases significantly.  $i_{pass}$  can be up to  $10^6$  times lower than  $i_{crit}$ , as indicated in figure 4.3.

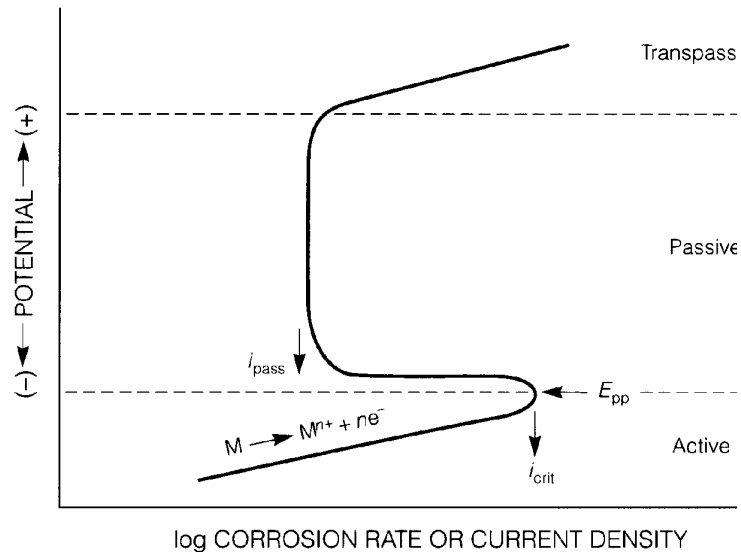


**FIGURE 4.3** Schematic active–passive polarization behavior.

At very high potentials the passive to transpassive transition occurs and the corrosion rate increases again. For stainless steel this potential is near the oxygen evolution potential, where the Cr rich passive film is unstable, as can be seen in the Pourbaix diagram. Going to higher  $H^+$  concentrations (higher acidity) and to higher temperatures leads to a decrease in the extend of the passive region, as shown in figure 4.4.

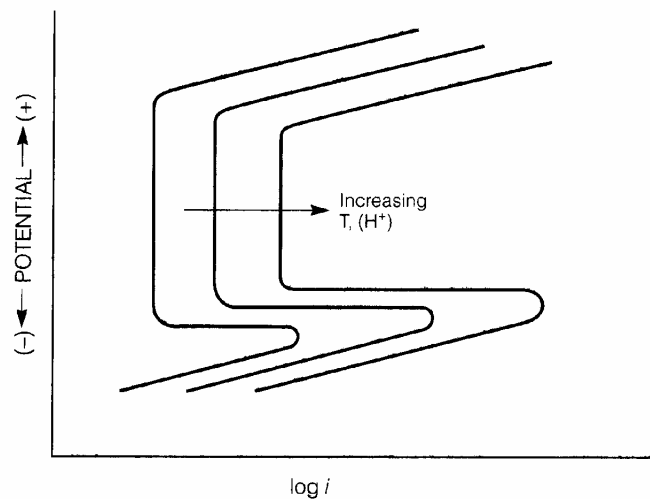


**FIGURE 4.4** Effect of increasing acid concentration and temperature on passivity.

#### Oxidizer Concentration Effects:

An increase in the oxidizer concentration increases the potential of the redox half cell reaction according to the Nernst equation. Taking mixed potential theory into account one can depict the effect of oxidizer concentration as shown in figure 4.5. The corrosion rate changes with

increasing oxidizer concentration from 1 to 8. The corresponding corrosion rates (current densities) are labeled A through F.

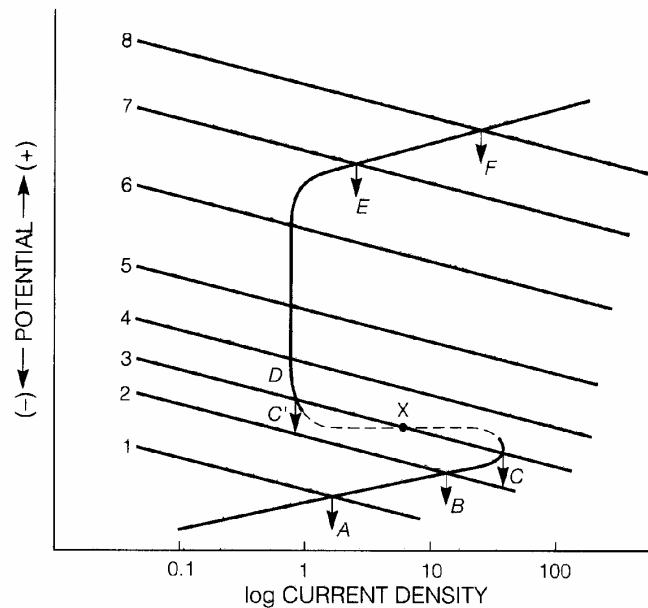


**FIGURE 4.5** Effect of oxidizer concentration on corrosion of an active-passive alloy.

From figure 4.5 one can make another plot with corrosion rate versus oxidizer concentration. In this case (figure 4.6) one can clearly see a hysteresis effect. This borderline passivity is an instable state, where any surface disturbance (scratching, stress, etc) will destabilize the passive film.

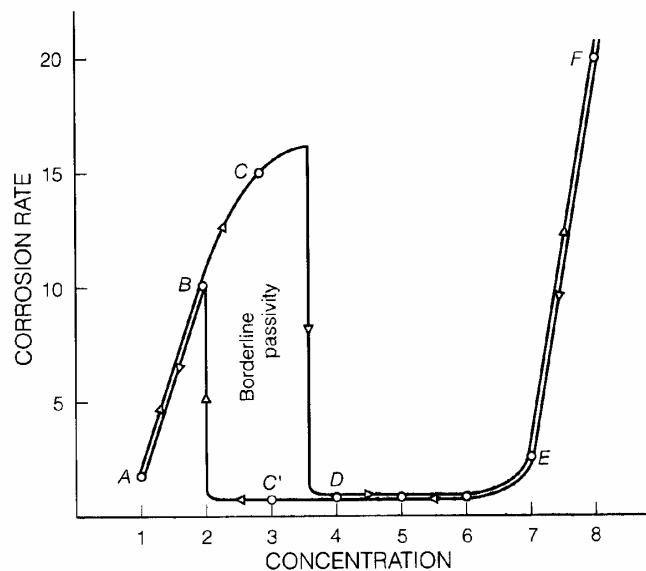
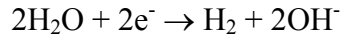


**FIGURE 4.6** Effect of oxidizer concentration on corrosion rate in an active-passive metal or alloy.

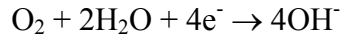
#### Solution Velocity Effects:

In a dilute salt solution (e.g. seawater) there is under deaerated conditions only one cathodic

reduction reaction available:



and therefore the metal corrodes in the active state. But the rate of hydrogen evolution is small and therefore the corrosion rate is small, too. If the solution becomes aerated, reduction of dissolved oxygen



starts to predominate as shown by line 1 in figure 4.7. In this case one has borderline passivity.

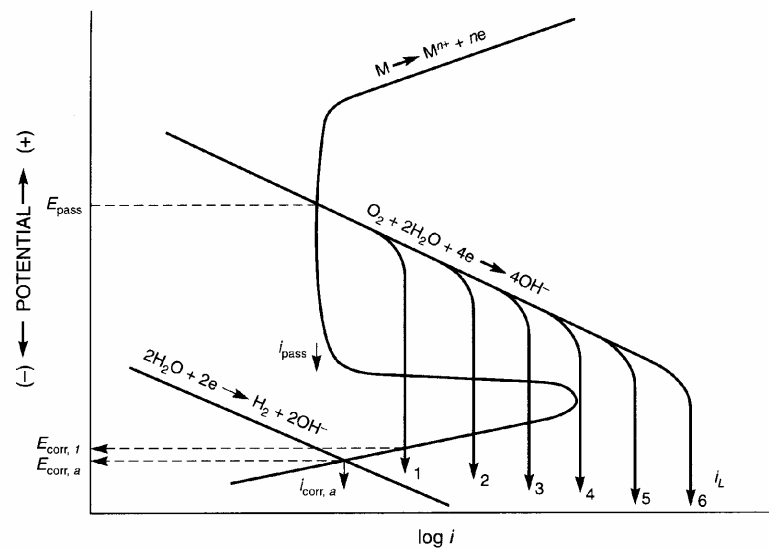


**FIGURE 4.7** Effect of deaeration, aeration, and stirring on corrosion of active-passive stainless steel in neutral saltwater.

But agitation of the solution leads to an increase in the limiting diffusion current from 1 to 6, and the system gets in the passive state. In figure 4.8 a the corrosion rate from figure 4.7 is plotted against the solution velocity (agitation). For comparison figure 4.8 b shows the same plot for a metal that does not form a passive film. There the corrosion only shifts from concentration to activation control.

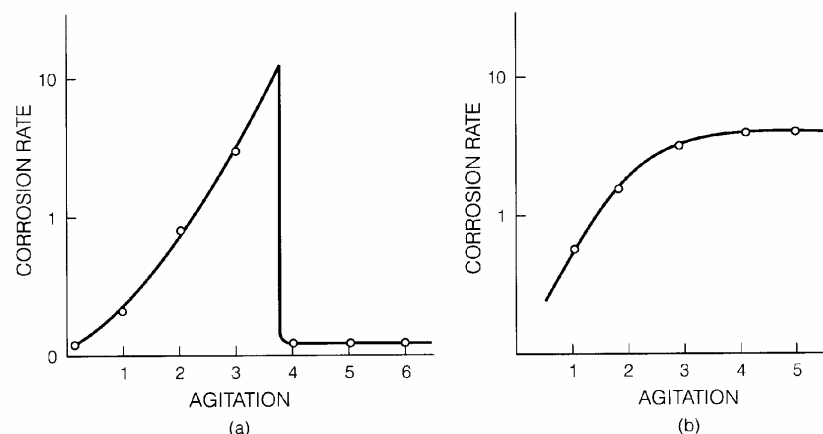


**FIGURE 4.8** Effect of stirring or solution velocity on corrosion rate for (a) active-passive stainless steel, derived from Figure 4.6, and (b) normal active metal, reproduced from Figure 3.13b.